A clock and wavefront mechanism for somite formation

R.E. Baker [a,*], S. Schnell [a,b,1], P.K. Maini [a]

[a] Centre for Mathematical Biology, Mathematical Institute, 24-29 St. Giles', Oxford OX1 3LB, UK
[b] Christ Church, Oxford OX1 1DP, UK

Abstract

Somitogenesis, the sequential formation of a periodic pattern along the antero-posterior axis of vertebrate embryos, is one of the most obvious examples of the segmental patterning processes that take place during embryogenesis and also one of the major unresolved events in developmental biology. In this article, we develop a mathematical formulation of a new version of the Clock and Wavefront model proposed by Pourquié and co-workers (Dubrulle, J., McGrew, M.J., Pourquié, O., 2001. FGF signalling controls somite boundary position and regulates segmentation clock control of spatiotemporal *Hox* gene activation. Cell 106, 219–232). Dynamic expression of FGF8 in the presomitic mesoderm constitutes the wavefront of determination which sweeps along the body axis interacting as it moves with the segmentation clock to gate cells into somites. We also show that the model can mimic the anomalies formed when progression of the wavefront is disturbed and make some experimental predictions that can be used to test the hypotheses underlying the model.
© 2006 Elsevier Inc. All rights reserved.

Keywords: Somitogenesis; Clock and Wavefront model; FGF8; Segmentation clock; Mathematical formulation

Introduction

Somites are formed as the result of a complex interaction of processes that take place in the early vertebrate embryo: a seemingly uniform field of cells is organised into discrete blocks via a mechanism which is tightly regulated both in space and time (Pourquié, 2003). Further differentiation of the cells within these somitic segments leads to the formation of the vertebrae, ribs and other associated features of the vertebrate musculature. Somitogenesis is one of the most well-studied examples of pattern formation in the developing embryo and is becoming, more and more, a leading candidate in developmental biology for a study that aims to couple findings at a molecular level with those at a cell and tissue level and lends itself openly to investigation from a more theoretical viewpoint (Schnell et al., 2002; Baker et al., 2003).

Somites are derived from two parallel bands of tissue known as the presomitic mesoderm (PSM) that lie alongside the notochord. At regular time intervals (every 90 min in the chick), a group of cells at the anterior end of the PSM undergo changes in their adhesive and migratory properties and coalesce together to form an epithelial block of cells known as a somite. Somites form in a strict AP sequence (Gossler and Hrabě de Angelis, 1998; Stickney et al., 2000; Stockdale et al., 2000), and budding of cells from the anterior part of the PSM compensates for the addition of cells at the posterior end of the PSM as the body axis lengthens. In this way, the PSM travels down the AP axis, remaining approximately constant in length throughout the process of segmentation and a wave of cell determination appears to sweep along the AP axis behind the PSM, leaving somites in its wake (Collier et al., 2000; Schnell et al., 2002).

Several genes are expressed dynamically in the PSM with cycling times equal to the time taken to form one somite (McGrew and Pourquié, 1998; Palmeirim et al., 1997). For example, during the formation of one somite, gene expression bands of *c-hairy-1* and *l-fng* sweep along the PSM: expression is considered to arise as a result of a segmentation clock acting within cells of the PSM.

* Corresponding author. Fax: +44 1865 270515.
  E-mail addresses: ruth.baker@maths.ox.ac.uk (R.E. Baker), schnell@indiana.edu (S. Schnell), maini@maths.ox.ac.uk (P.K. Maini).
  [1] Present address: Indiana University, School of Informatics and Biocomplexity Institute, Eigemann Hall 906, 1900 East 10th Street, Bloomington, IN 47406, USA.

Another gene with dynamic expression in the PSM is fgf8. High transcription levels of *fgf8* occur in the posterior-most part of the PSM (Dubrulle and Pourquié, 2004) which generates an FGF8 gradient with elevated signalling levels in the posterior PSM decreasing in a graded fashion with movement in the anterior direction (Dubrulle and Pourquié, 2002, 2004). As the axis elongates, the wavefront of FGF8 moves in a posterior direction so that signalling levels remain constant relative to the moving PSM. Cells move up through the PSM as development proceeds so that cells are initially part of the region where FGF8 signalling prevails and begin to experience lower levels of FGF8 as the gradient recedes.

Dubrulle and co-workers have shown that the different levels of FGF8 in the PSM coincide with regions of differing structure: in the posterior-most two-thirds of the PSM where FGF8 signalling is high, cells are arranged in a loose mesenchymal manner, whereas in the anterior-most third where FGF8 signalling is low, cell arrangement has become more compact and the epithelialisation process underlying somite formation has already begun (Dubrulle et al., 2001).

Besides the obvious structural differences between tissue found in the different regions of the PSM, there are also disparities between levels of segmental determination (Dubrulle et al., 2001). Determination refers to the irreversible commitment of a cell to a particular developmental pathway.

The border which separates the two regions of FGF8 signalling is known as the *determination front*. It has been found that "FGF8 is sufficient to maintain the caudal identity of presomitic mesoderm cells and that down-regulation of FGF8 signalling at the level of the determination front is required to enable cells to proceed further with the segmentation process" (Dubrulle et al., 2001). Fig. 1 is an illustration of the vertebrate body plan during somite formation with the determined and undetermined regions clearly marked.

Perturbation of the FGF8 signalling wavefront has been investigated experimentally by implanting a heparin bead soaked in FGF8 alongside the PSM. FGF8 diffuses out from the bead along the PSM, and the effect of this is to displace the determination front from its normal position. The result is the formation of abnormally small somites on the side of the embryo on which the bead is grafted, extending for a distance of up to 6–7 somites rostral to the bead with one abnormally large somite forming caudal to the bead such that the sequence of affected somites falls back into register with the control side (Dubrulle et al., 2001).

Previous models

Several models have already been suggested for somitogenesis: Cooke and Zeeman's original Clock and Wavefront model (Cooke and Zeeman, 1976); Meinhardt's Reaction-Diffusion model (Meinhardt, 1986); and Stern's Cell Cycle model (Stern et al., 1988; Primmett et al., 1988; Primmett et al., 1989), to name but a few. The models named above have been reviewed by the authors in Baker et al. (2003) and therefore we only discuss them briefly here.
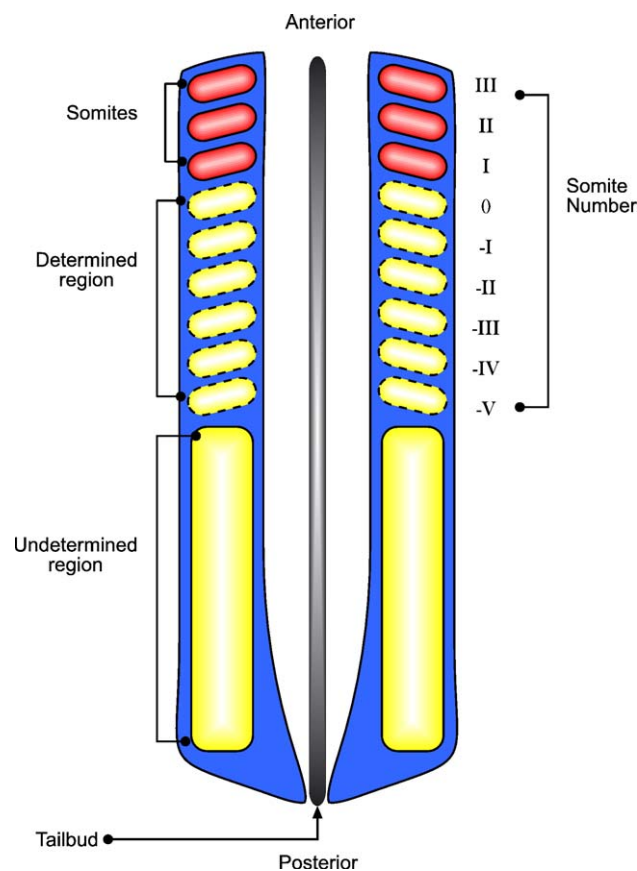

Fig. 1. An illustration of the vertebrate body plan during somite formation. The red blocks denote individual somites, the yellow blocks denote the determined region of cells with its pre-pattern of somites and the yellow bands represent the undetermined regions of the PSM. There is a determination front at the level of somite -V which divides the PSM into two distinct regions; the pre-patterned region where the epithelialisation process has begun (low FGF8 signalling) and the spatially homogeneous region where the cells are still in an immature state (high FGF8 signalling).

Cell Cycle model

The Cell Cycle model of Stern and co-workers (Stern et al., 1988; Primmett et al., 1988, 1989) assumes that cells are arranged along the AP axis such that their cell cycles are in synchrony. Cells in the anterior PSM being further advanced through the cycle than cells in the posterior PSM. Segmentation occurs when cells reach a certain time window in their cell cycle. A mathematical formulation of the Cell Cycle model was first proposed by Collier et al. (2000).

The hypotheses underlying the Cell Cycle model are now widely disputed. Palmeirim and co-workers have argued against the role of the cell cycle as a segmentation clock based on the cycling times of *c-hairy-1* in the PSM (Palmeirim et al., 1997) and the model cannot explain the effects of local application of FGF8 (Dubrulle et al., 2001). However, the mathematical basis of the model is that of a signalling process, with control of the signal and its subsequent actions being determined by external factors: with suitable modifications, it can still be applied to study somitogenesis.

Reaction-Diffusion model

Meinhardt's Reaction-Diffusion model assumes that cells can be in one of two possible states, *a* or *p*, which correspond to the anterior and posterior phenotypes of the somite. The *a* and *p* states are such that they locally exclude each other but stimulate each other over a long range. Cells switch from one state to another until they reach a stable state. In this way, a pattern of stable *apap...* stripes is formed (Meinhardt, 1986), corresponding to the observed pattern of division of somites into anterior and posterior halves: each *ap* segment constitutes a somite.

The wavefront of FGF8 provides the positional information gradient needed to generate the pattern, and further evidence for Meinhardt's model comes from the confined expression of *c-hairy-1* to the posterior half of the somite (Dale and Pourquié, 1997). In fact, the Reaction-Diffusion model is the only one to address anterior/posterior somite subdivision. However, in its present form, the Reaction-Diffusion model cannot explain the effects of local FGF8 application.

Clock and Wavefront model

The Clock and Wavefront model was first proposed by Cooke and Zeeman (1976). The model postulates the existence of a longitudinal *positional information* gradient down the AP axis of vertebrate embryos, which interacts with a smooth cellular oscillator (the clock), to set the time in each cell at which it will undergo a *catastrophe*. By catastrophe, they mean a rapid change of state, which could possibly be the rapid change in locomotory and adhesive behaviour of cells when they form somites.

The wavefront of FGF8 provides a likely candidate for the longitudinal positional information gradient, and there is wide evidence for the segmentation clock. However, the model has not been formulated mathematically. In this article, we employ a signalling process similar to that developed for the Cell Cycle model as a rigorous framework for the Clock and Wavefront model.

Aims and outline

The specific version of the Clock and Wavefront model considered in this article is that proposed by Pourquié and co-workers (Dubrulle and Pourquié, 2002; Pourquié, 2004a). Our goal is to investigate the consequences of the interaction between the clock and the wavefront in response to experimental perturbations. We do not aim to model specifically the mechanisms underlying the clock nor the wavefront. However, we note that the FGF8 signalling gradient along the PSM provides a biological basis for a wavefront and the periodic, dynamic expression of genes such as *c-hairy-1* and *l-fng* provides evidence for the presence of a segmentation clock.

In the following section, we detail a "word" model which is accompanied by a mathematical formulation (see Appendix A) based on the previous model of Maini and co-workers (Collier et al., 2000; Schnell et al., 2002; McInerney et al., 2004). We demonstrate that this new model can produce a coherent pattern of somites which are regulated both temporally and spatially.

We then extend our model to include the effects of local application of FGF8, presenting both a schematic view of the resulting anomalies and numerical simulation of the accompanying mathematical model. Finally, we present some experimentally testable predictions that may be used to verify the validity of our model and discuss the need for estimation of the parameter values involved in the model.

A new Clock and Wavefront model for somite formation

The Clock and Wavefront model proposed by Pourquié and co-workers (Dubrulle and Pourquié, 2002; Dubrulle et al., 2001; Pourquié, 2004a) hypothesises that there is some interaction between the wavefront of FGF8 and the segmentation clock in the PSM that acts to gate cells into potential somites. For a cell at a particular point, they assume that competence to segment will only be achieved once FGF8 signalling has decreased below a certain threshold. The threshold level of FGF8 is the level expressed at the determination front (Dubrulle and Pourquié, 2002).

To develop a mathematical formulation of Pourquié's Clock and Wavefront model, we constructed a system of equations in which the segmentation clock controls *when* the boundaries of the somites will form and the determination front controls *where* they form. This is in agreement with Dubrulle and co-workers' observations (Dubrulle et al., 2001; Tabin and Johnson, 2001). In addition, we introduce the following assumptions:

1. Once cells have reached the determination front, they become competent to segment by gaining the ability to respond to a chemical signal and produce a somitic factor.
2. At a certain time t_s later, they become able to signal. t_s is equal to the period of the segmentation clock, which is coincident with the period of the cycling genes.
3. Once a cell has reached the determination front, it will change its response to FGF8; essentially, we will assume that it becomes refractory to FGF8 signalling.

This model is based on the signalling model presented by Maini and co-workers (Collier et al., 2000; Schnell et al., 2002; McInerney et al., 2004): at a certain time, a small fraction of cells at the anterior-most end of the PSM will gain the ability to signal, that is, they would have reached the determination front at a time t_s previously. These *pioneer cells* will produce and emit a signal which will diffuse along the PSM. Any cell which has reached the determination front, and therefore becomes competent to segment, would respond to such a signal by increasing its adhesion to neighbouring cells which are responding in a similar manner, thereby forming a potential somite. At this point, a cell has been specified as somitic, and it will go on to segment and form part of a somite during subsequent oscillations of the segmentation clock. The process begins again once the new pioneer cells at the anterior edge of the PSM become competent to signal. Emission of the signal is transient due to negative feedback on signal production by the cells which react to the signal. This feedback loop results in periodic pulses in the signal and hence the specification of

somites at regular time intervals. Fig. 2 illustrates the vertebrate body plan during somite formation as envisaged by the new Clock and Wavefront model. The interaction of the segmentation clock with the determination front is clearly shown.

It should be noted at this point that the clock used in our model does not have an immediate correspondence with outputs of the segmentation clock observed experimentally by Pourquié and others (Dale et al., 2001; McGrew et al., 1998; Palmeirim et al., 1997; Saga and Takeda, 2001). We do not doubt this large body of evidence regarding gene oscillation in the PSM, and we explore this point more thoroughly in the Discussion.

The mathematical model constructed from Pourquié's descriptive Clock and Wavefront model consists of a coupled system of three non-linear partial differential equations. The state variables which the system describes will be a *somitic factor* which is integral in determining the fate of cells (a cell will only go on to form part of a somite once it has produced a high enough level of somitic factor), a *diffusive signalling molecule* which is produced by the pioneer cells at the anterior-most end of the PSM and finally a generic *FGF8 molecule* which is able to confer the ability of cells to produce somitic factor and signal (according to their level of expression of FGF8). The complete system of equations is outlined in Appendix A.

We know that whilst Hensen's node is regressing along the AP axis, cells are left behind and incorporated into the PSM with a certain level of *fgf8* which decays over time. FGF8 is translated by these cells and this creates the signalling gradient. We choose to model this complex phenomenon by assuming that FGF8 is produced only in the tail and that it diffuses out from the tail
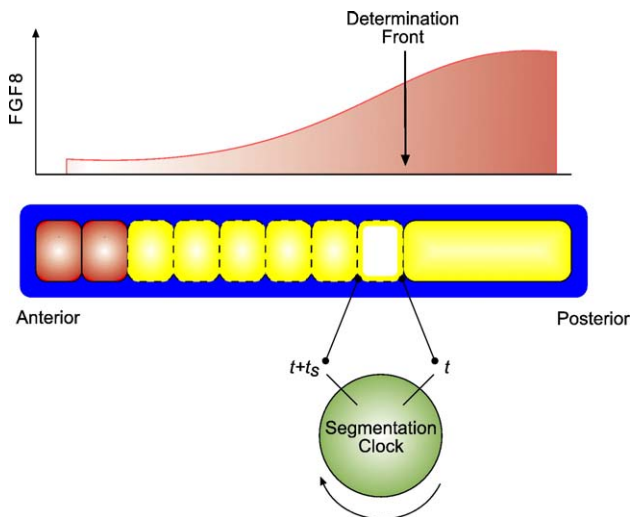

Fig. 2. Diagrammatic representation of the vertebrate body plan during somite formation within Pourquié's Clock and Wavefront model. In the top part of the diagram, the FGF8 wavefront is illustrated together with the position of the determination front. The middle section of the diagram shows the AP axis of the embryo with the somites (red blocks), determined region and its pre-pattern (yellow blocks) and the undetermined PSM (yellow band) clearly marked. The bottom part of the diagram shows the segmentation clock with the time t at which a cell reaches the determination front and the time t_s later at which it becomes competent to signal. The hollow yellow block marks the position of the next somite to be specified: the posterior boundary is fixed by the position of the determination front at the time at which pioneer cells at the anterior boundary produce a signal.

along the PSM and undergoes linear decay (see Baker et al. (in press) for more details). The result is the formation of an FGF8 gradient similar to that shown in Fig. 3(a). The FGF8 gradient moves in a posterior direction along the PSM and confers the ability upon cells to produce a somitic factor; at time t_s later, they gain the ability to signal. Somitic factor production is activated in response to a pulse in the signal emitted from the pioneer cells at the anterior end of the PSM. Rapid inhibition of signal production by the somitic factor ensures that peaks in signal concentration are transient and produced at regular intervals (see McInerney et al., 2004 for further details).

We can anticipate the pattern of somites formed using our model by considering the progress of the points P_u and P_v which measure the times at which cells become competent to produce somitic factor and signalling molecule (respectively). In a control case, the determination front remains at a constant axial position relative to the PSM and hence moves down the AP axis at a constant speed. Cells gain the ability to produce signalling molecule a time t_s after they become competent to produce somitic factor. Therefore, the number of cells with the ability to segment and the number of cells able to produce signalling molecule increase at a constant rate. Fig. 4 illustrates the progress of P_u and P_v along the AP axis and also the expected pattern of somites formed. In this example, at $t = 0$, cells at $x = 1$ become the next set of pioneer cells and also become competent to produce somitic factor. At time $t = 2$, these pioneer cells become competent to produce the diffusive signalling molecule, and they send out a signal. All cells between $x = 1$ and $x = 2$ have now reached the determination front and are able to respond to this signal by producing somitic factor. These cells between $x = 1$ and $x = 2$ produce somitic factor in a coherent manner, thereby committing themselves to form a somite together. It is encouraging to note from Fig. 4 that somites are regular in size and form at regular intervals.

We also solved our mathematical formulation of the model (see Appendix A) numerically using the NAG library routine D03PCF (see Appendix B for more details). Fig. 5 shows the results of the numerical computation: the top panel shows the dynamics of the somitic factor, the middle panel shows the dynamics of the signalling molecule and the bottom panel shows the dynamics of FGF8. We see that the region of high FGF8 expression moves in a posterior direction along the AP axis with constant speed. A sequence of successive signals, moving in a posterior direction, produces a series of coherent rises in the level of somitic factor which then enables cells to progress to form discrete somites. We note, once again, that our model predicts a spatially uniform series of somites forming at regular time intervals.

Local application of FGF8

Earlier in this work, we detailed the experiments of Dubrulle and co-workers regarding local perturbation of FGF8 in the PSM (Dubrulle et al., 2001). A source of FGF8 implanted in the PSM caused somite anomalies as a result of a disturbance in the progression of the determination front. We incorporate this into our model by assuming that FGF8 is not only produced in the
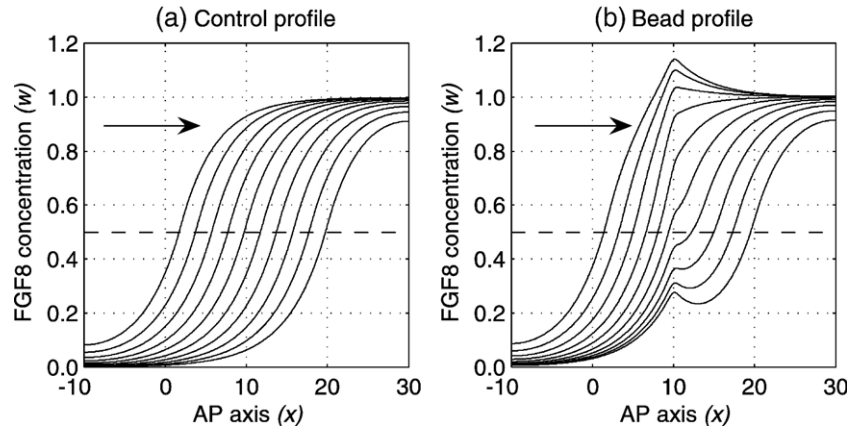
Fig. 3. Numerical solution for the FGF8 profile along the AP axis. In each graph, the solution is plotted for $t = 4, 8, 12, 16, 20, 24, 28, 32, 36$ and 40 (indicated by arrows) and the hypothetical level of FGF8 marking the determination front is indicated by the dashed line. (a) In a control embryo, the position of the determination front moves with constant speed down the AP axis. (b) A bead soaked in FGF8 is implanted at $x = 10.0$ resulting in perturbation of the determination front: in a region ahead of the bead, progression of the determination front slows, whilst behind the bead the rate of progression of the determination front increases. The anterior end of the PSM lies on the left-hand side (LHS) of the figure and the posterior end on the right-hand side (RHS). Parameters are as follows: $\eta = 1.0$, $D_w = 50$, $\xi = 0.5$, $x_b = 0$ and $\phi = 5.0$.

tail region of the embryo, but also via a small source of FGF8 implanted at a constant axial level (see Appendix C for details of the extended mathematical model). Solving numerically the new equations for the FGF8 signalling dynamics results in the FGF8 profile shown in Fig. 3(b). The dashed line indicates the progression of the determination front, and we see that its
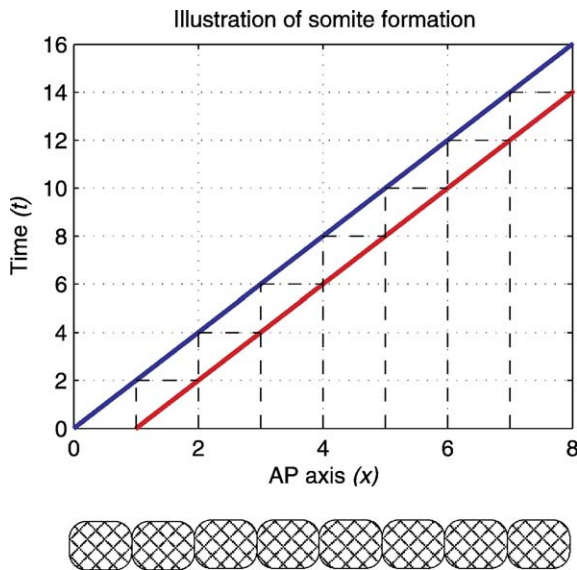

Fig. 4. Illustration of the manner in which somites are formed in the new Clock and Wavefront model. In the top diagram, the positions of successive somites are found by tracing the lines as shown. The diagonal lines indicate the positions of the points P_u (red) and P_v (blue). Pioneer cells, at $x = 0, 1, 2,...$, send out signals, at times $t = 0, 2, 4,...$ respectively. Cells which have reached the determination front are able to produce somitic factor (those between $x = 0$ and $x = 1$, between $x = 1$ and $x = 2$, etc.) and they do so in a coherent manner, thereby forming a somite together. The bottom diagram illustrates the relative somite sizes. The reciprocal of the gradient of the lines representing P_u and P_v is a measure of the speed at which somites are formed and the period of the clock is $t_s = 2.0$. The anterior end of the PSM lies on the LHS of the figure and the posterior end on the RHS.

progression slows ahead of the bead whilst it increases behind the bead.

In Fig. 6, we use the same method as before to plot the patterns of somites that could arise as a result of local application of FGF8. The top panel shows the results when a weak source of FGF8 ($\phi = 3.0$) is implanted alongside the PSM: the lines representing P_u and P_v deviate slightly from their control paths and the result is a series of slightly smaller somites forming anterior to the bead where the progression of the determination front is slowed and a large somite posterior to the bead where the progression of the determination front has increased. We note that somite formation falls back in line with the control case within one or two somites distance posterior to the bead.

The middle panel shows the results of our model when a slightly stronger source of FGF8 ($\phi = 6.0$) is implanted alongside the PSM: in this example, the anomalies produced are more marked, and we see a sequence of 6–7 small somites forming anterior to the bead and a very large somite forming posterior to the bead. Once again, somite formation falls back into register both spatially and temporally with the control embryo pictured in Fig. 4.

Finally, the bottom panel of Fig. 6 shows the results of local application of a very strong source of FGF8 ($\phi = 9.0$). This could correspond to the source being implanted inside the PSM rather than alongside it. This case differs from the others shown in this figure as it results in a region of the PSM that will never segment: the level of FGF8 produced in a region surrounding the bead is high enough to ensure that cells in this region will never have sufficiently low levels of FGF8 to reach the determination front and hence never be able to produce somitic factor. We see a sequence of small somites in a region anterior to the bead followed by a region where the cells remain unsegmented followed by a large somite posterior to the bead and then normal segmentation.

It is encouraging to note that all three of the cases pictured in Fig. 6 have been observed experimentally (Dubrulle et al.,
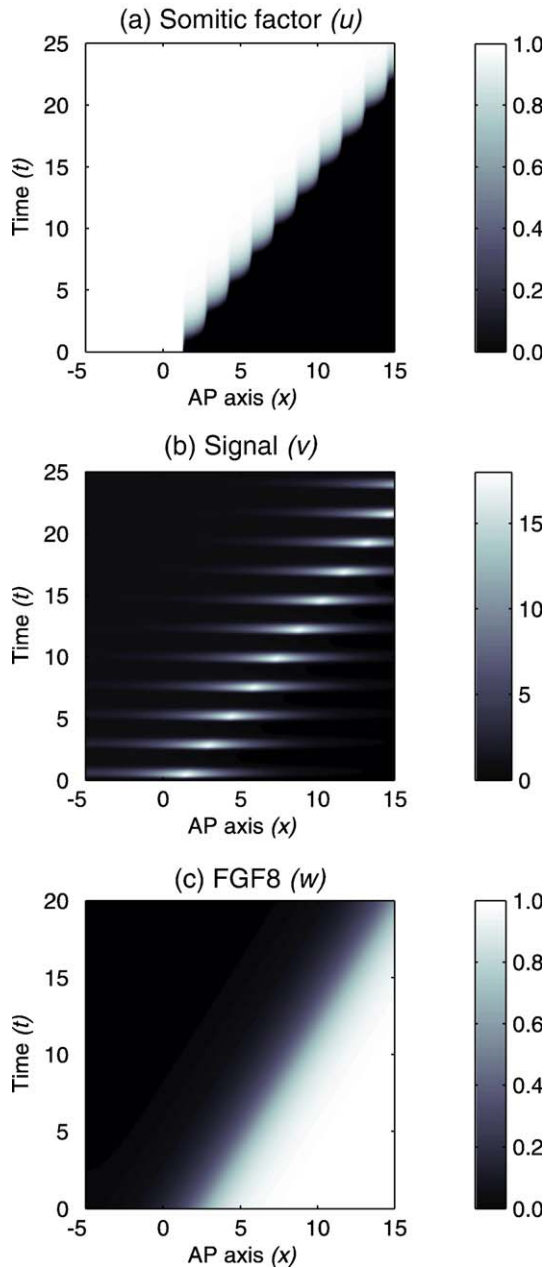
Fig. 5. Numerical solution of the new mathematical formulation of the Clock and Wavefront model for somite formation showing the spatio-temporal dynamics of the somitic factor (a), the signalling molecule (b) and FGF8 (c). The anterior end of the PSM lies on the LHS of the figure and the posterior end on the RHS. Parameters are as follows: $\mu = 10^{-4}$, $\gamma = 10^{-3}$, $\kappa = 10$, $\varepsilon = 10^{-3}$, $\eta = 1.0$, $D_v = 50$, $D_w = 20$, $x_n = 0.0$, and $c_n = 0.5$.

formation: perturbing the speed at which the determination front progresses along the AP axis and perturbing the period of the segmentation clock. Using our model, we would expect to find results in vivo similar to those seen in Fig. 8.

Increasing the period of the segmentation clock (whilst keeping regression of the determination front constant) would result in increased somite size: when the pioneer cells at the
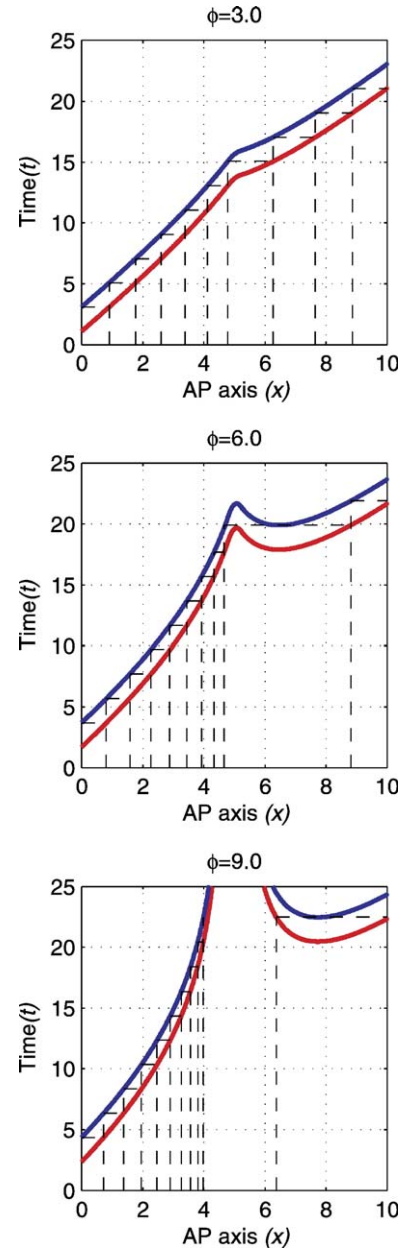

Fig. 6. The progress of P_u and P_v as ϕ, the strength of the bead source, is varied. The red line depicts the progress of P_u and therefore the time at which cells reach the determination front and become able to produce somitic factor. The blue line depicts the progress of P_v and shows the time at which cells become able to send out a signal. The boundaries of the presumptive somites are marked by the dashed lines. As previously, the positions of the somite boundaries are found by tracing between the two lines. The anterior end of the PSM lies on the LHS of the figure and the posterior end on the RHS. Parameters are as follows: $\eta = 1.0$, $D_w = 10$, $x_n = 0.0$, $c_n = 0.5$, $x_b = 5.0$, $\xi = 0.2$, $t_s = 2.0$ and $F = 0.5$. See Baker et al. (in press) for more details.

2001). Fig. 7 shows a typical numerical simulation of the mathematical model corresponding to the middle panel of Fig. 6. Note the extra large somite.

Experimental predictions

In order to test the validity of Pourquié's Clock and Wavefront model, it is necessary to make some experimentally testable predictions. First, we investigate two of the more (mathematically) simple ways in which to perturb somite
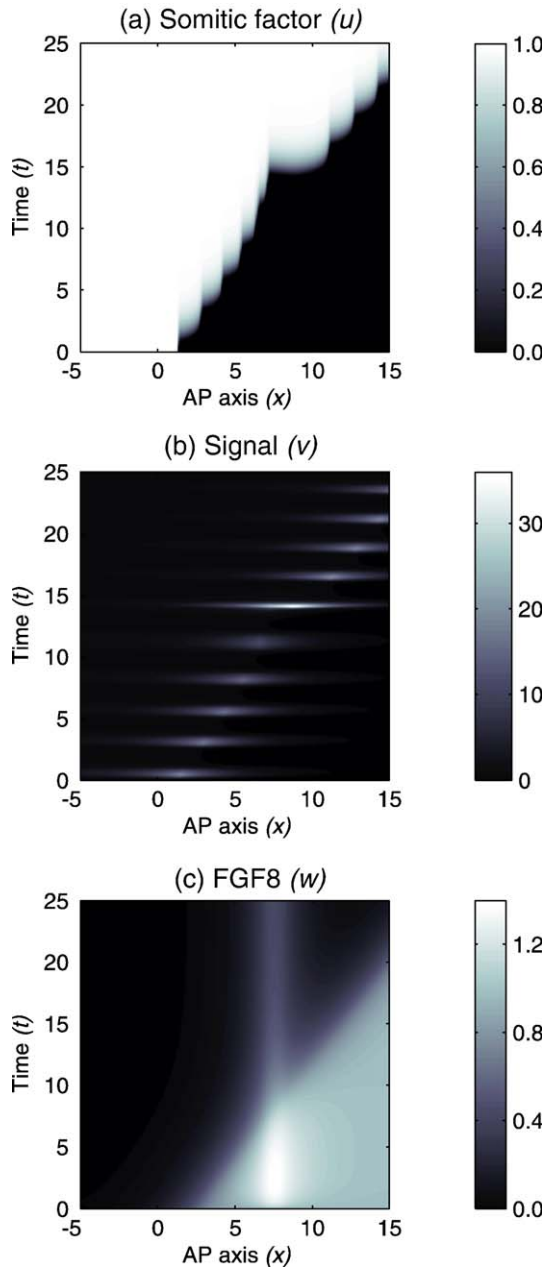
Fig. 7. Numerical solution of the new Clock and Wavefront model for somite formation showing the spatio-temporal dynamics of the somitic factor (a), the signalling molecule (b) and FGF8 (c). With a source of FGF8 implanted in the PSM, the somite anomalies are obvious. The anterior end of the PSM lies on the LHS of the figure and the posterior end on the RHS. Parameters are as follows: $\mu = 10^{-4}$, $\gamma = 10^{-3}$, $\kappa = 10$, $\varepsilon = 10^{-3}$, $\eta = 1.0$, $\phi = 1.5$, $D_v = 50$, $D_w = 20$, $x_n = 0.0$, $c_n = 0.5$, $x_b = 50$ and $\xi = 0.5$.

anterior end of the PSM become competent to produce a signal, more cells would have reached the determination front (consider Fig. 2) and become able to segment. This is shown in Fig. 8(a).

Decreasing the rate at which the determination front is regressing (whilst keeping the period of the segmentation clock constant) would result in the determination front moving a shorter distance during one oscillation of the segmentation clock than it would in the control case. The result of this would

be less cells gaining the ability to segment and hence smaller somites. This is depicted in Fig. 8(b).

The third prediction we make is regarding inhibition of FGF8 in the PSM. There have been some preliminary experiments to investigate the effect of inhibiting the FGF8 signalling gradient in the PSM (Dubrulle et al., 2001). Upon treatment with SU5402, a drug known to specifically block the kinase activity of FGF8 receptors, embryos formed with a large pair of somites at the level of somite -IV at the time of application of SU5402. We can explain the formation of this anomalous somite by reasoning that the SU5402 treatment decreases the level of FGF8 signalling throughout the PSM, resulting in a posterior shift of the determination front and an anomalous somite. SU5402 is rapidly degraded, and it is expected that FGF8 signalling is only affected during a time frame approximately equal to the time taken to form one somite (Pourquie, 2004b). Degradation of SU5402 would result in an increase in FGF8 signalling activity, back to the original undisturbed level. We model this
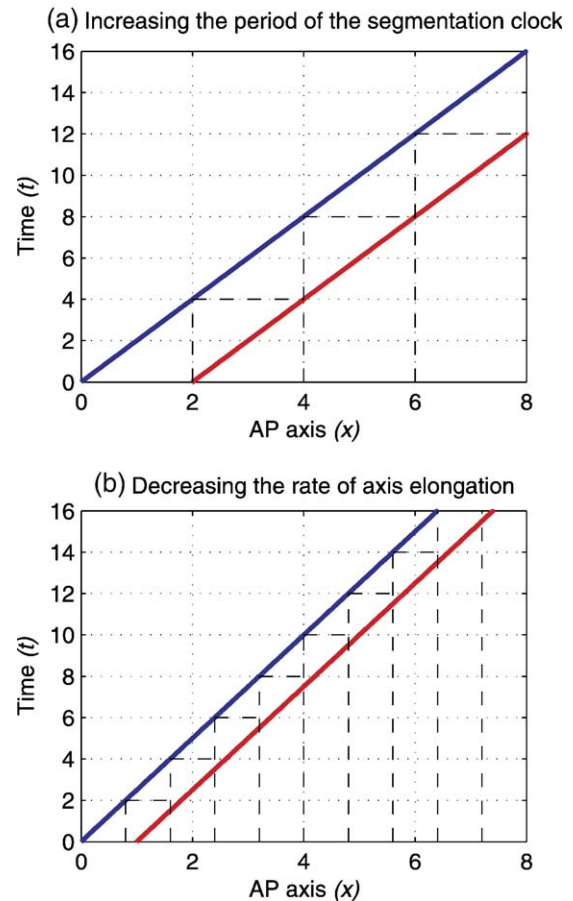

Fig. 8. (a) Increasing the period of the segmentation clock ($t_s = 4.0$) results in larger somites. (b) Decreasing the rate of determination front progression (whilst keeping the period of the segmentation clock constant, $t_s = 2.0$) results in smaller somites. The red line depicts the progress of P_u and therefore the time at which cells reach the determination front and become able to produce somitic factor. The blue line depicts the progress of P_v and shows the time at which cells become able to send out a signal. The boundaries of the presumptive somites are marked by the dashed lines. As previously, the positions of the somite boundaries are found by tracing between the two lines. The anterior end of the PSM lies on the LHS of the figure and the posterior end on the RHS.

mathematically by introducing a sink term into our equation for FGF8 which is active for a certain period and proportional to the amount of FGF8 present in the PSM.

We can use similar methods to those used throughout the rest of this paper to estimate the anomalies formed when SU5402 is used to inhibit FGF8 signalling. Fig. 9(a) shows the anomalies produced when FGF8 signalling is inhibited for a brief period: a large somite forms at $t = 6.0$ and normal segmentation is seen thereafter. Fig. 9(b) shows the anomalies produced when FGF8 signalling is inhibited for a longer period: a smaller somite forms posterior to the larger somite. We note that, should FGF8 be inhibited for an even longer period, our model would predict the formation of a large somite, followed by a series of normal somites, followed by a small somite and then normal segmentation.

The results generated by numerically solving the mathematical model are shown in Fig. 10. SU5402 is injected at time $t = 8.5$, and we assume that the effects last until time $t = 9.5$. We
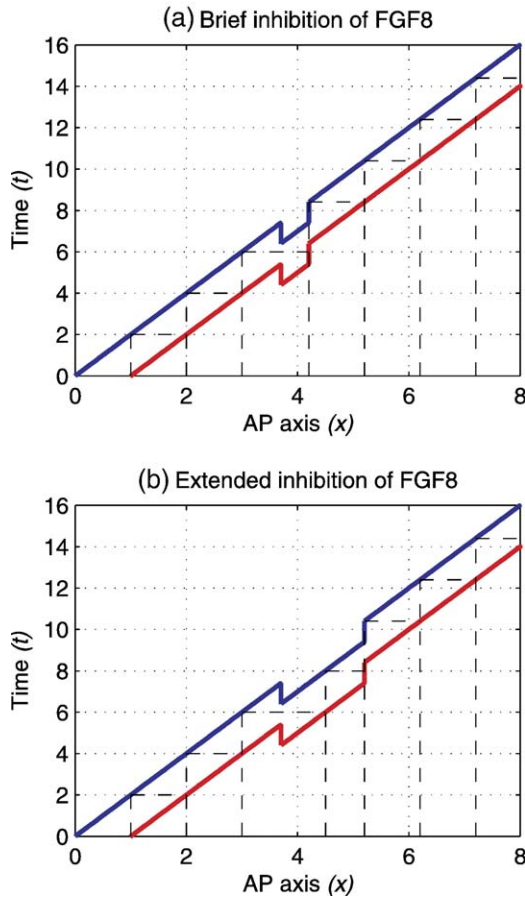

Fig. 9. Inhibition of FGF8 signalling results in somite anomalies. (a) Case in which SU5402 is assumed to act for a brief period (less than the period of the segmentation clock). (b) Case in which FGF8 is assumed to be inhibited for a longer period. The red line depicts the progress of P_u and therefore the time at which cells reach the determination front and become able to produce somitic factor. The blue line depicts the progress of P_v and shows the time at which cells become able to send out a signal. The boundaries of the presumptive somites are marked by the dashed lines. As previously, the positions of the somite boundaries are found by tracing between the two lines. The anterior end of the PSM lies on the LHS of the figure and the posterior end on the RHS. In both cases, the period of the clock is $t_s = 2.0$.
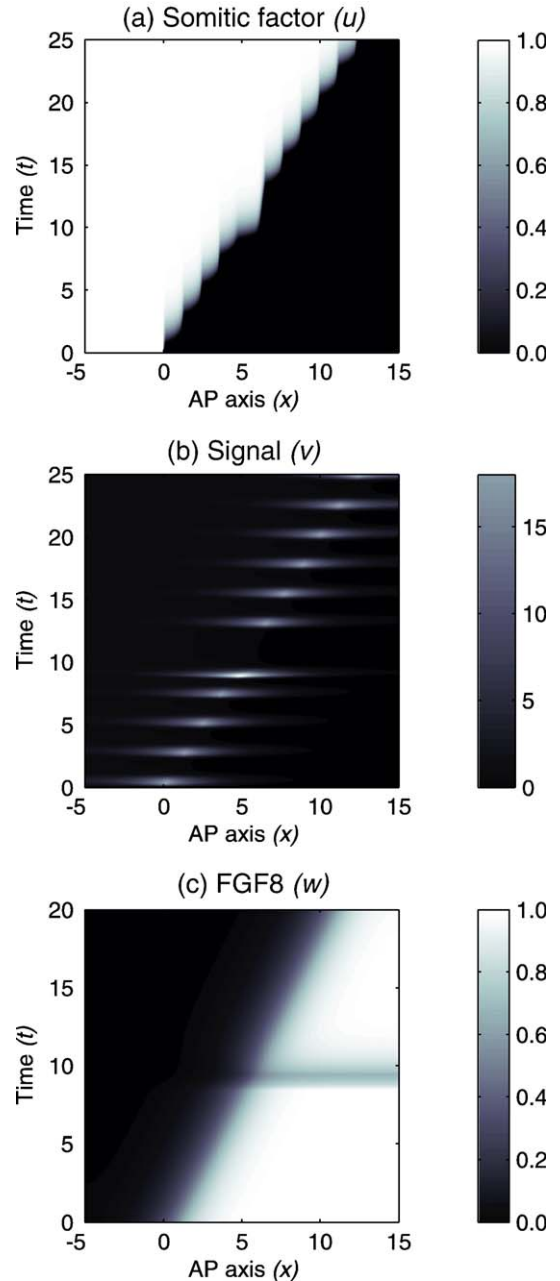

Fig. 10. Numerical solution of the new mathematical formulation of the Clock and Wavefront model for somite formation showing the spatio-temporal dynamics of the somitic factor (a), the signalling molecule (b) and FGF8, (c). With inhibition of FGF8 signalling using SU5402, we see the formation of a large somite at the level of the determination front at the time the drug is applied ($t = 8.5$ until $t = 9.5$). The anterior end of the PSM lies on the LHS of the figure and the posterior end on the RHS. Parameters are as follows: $\mu = 10^{-4}$, $\gamma = 10^{-3}$, $\kappa = 10$, $\varepsilon = 10^{-3}$, $\eta = 1.0$, $D_v = 50$, $D_w = 20$, $x_n = 0.0$, $c_n = 0.5$, $x_b = 5.0$ and $\xi = 0.5$.

see the corresponding decrease in FGF8 signalling throughout the PSM in Fig. 10(c). The posterior shift in the determination front as a result of SU5402 application causes the fifth signal and fifth somite to be generated early, and the fifth somite is larger than normal. Rapid degradation of SU5402 results in the determination front re-assuming its normal position and segmentation patterns returning to normal.

Parameter estimation

In order to make quantitative predictions for the somite anomalies produced when FGF8 expression is perturbed, it will be necessary to have accurate estimates of the parameters involved, more specifically, the rate at which FGF8 is able to diffuse along the PSM and its rate of decay in relation to the speed of axis elongation and, correspondingly, somite formation.

In experiments in which FGF8 is perturbed locally by implantation of a bead alongside the PSM, it is uncertain how much of the diffusing FGF8 is actually able to enter the PSM and affect somite formation. Our model does not take this into account, but it may be possible to match the anomalies seen experimentally under different concentrations of bead source with the anomalies produced by the mathematical model. In this way, it may be possible to estimate the amount of FGF8 entering the PSM from the severity of the anomalies produced. Before this can happen however, we need accurate estimation of the rate at which FGF8 is able to diffuse along the PSM and its rate of decay.

Discussion

In this paper, we have presented a revised version of Pourquié's Clock and Wavefront model for somitogenesis with a mathematical basis derived from the models by Maini and co-workers (Collier et al., 2000; Schnell et al., 2002; McInerney et al., 2004). We combine outputs from the FGF8 wavefront and the segmentation clock to control the signalling process described by the mathematical model.

We next moved to extend this mathematical model to include the effects of local perturbation of FGF8. We represented a heparin-soaked bead implanted alongside the PSM by a constant production term for FGF8, which is confined to a small region of the AP axis. In a similar manner, we solved the revised equation for FGF8 expression numerically and demonstrated the displacement of the determination front from its conventional path.

In both the control case and the perturbed cases, we were able to demonstrate the ability of our model to produce the results seen in vivo; progression of the determination front along the AP axis conferred upon cells the ability to produce a series of signals with the centre of the pulse travelling posteriorly along the AP axis, leaving a series of coherent somites in their wake. The control case produced a series of uniform somites and the perturbed cases a series of abnormal somites with the intensity of the somite anomalies produced mirroring the severity of the disturbance in the FGF8 profile.

We also note at this stage that it is likely that the effects of local application of FGF8 via a heparin-soaked bead will wear off before all the PSM that would otherwise be affected by this perturbation can be gated into somites (Pourquie, 2004b). Decaying effects of local application of FGF8 could result in pronounced "large" somite anomalies as decay of the source would confer the potential to become somitic to very many cells at the same time. The effects of a temporally varying local source of FGF8 is something that remains to be investigated.

The results of this work clearly show that perturbation of somitogenesis leads to the incorporation of certain cells into differently numbered somites than their control counterparts. It can be seen that such cells will go on to segment within a different time step and will therefore experience a different number of clock oscillations before segmenting (Tabin and Johnson, 2001). Dubrulle et al. (2001) demonstrate that "FGF8 treatment can increase the number of clock oscillations experienced by PSM cells without altering their absolute axial position in tissue. Cells which experience an extra oscillation become incorporated into a differently numbered somite and exhibit *Hox* expression indicative of a more posterior fate when compared with contralateral control cells." Our model clearly accounts for this result (compare Figs. 4 and 6).

Lastly, we have chosen to simplify the clock: removing its complexity by modelling it as a signalling process. We note that the clock present in our model does not correspond to the most commonly observed somitogenesis *cycling genes* (Dale et al., 2001; McGrew et al., 1998; Palmeirim et al., 1997; Saga and Takeda, 2001), which have been widely accepted as constituting the segmentation clock. Expression of such genes begins as a wide stripe in the posterior PSM: the stripe travels in an anterior direction, narrowing as it moves, until it comes to rest in the newly forming somite. However, genes such as *l-fng* and *c-hairy-1* are readouts from the segmentation clock, and although these genes and their role in somitogenesis have been widely documented, the mechanisms underlying the segmentation clock are still far from being completely understood. There has been some progress in modelling aspects of the clock (see for example Lewis, 2003; Monk, 2003), but these are early models and we do not feel that incorporation of the mechanisms considered by these authors into our model would allow us to shed any further light on the aspects of somitogenesis considered here. It is for these reasons that we choose to simplify the clock, removing its enormous complexity by modelling it as a signalling process, with control of the somite pattern held by a combination of this process and the FGF8 wavefront. It is interesting to note, however, that recent experiments of Ishikawa et al. (2005) have identified a gene, *nkd1*, which could be linked to our signalling molecule, *v. nkd1* oscillates in the PSM with the same period as the other cycling genes, but it is only expressed in anterior regions of the PSM.

In a sister paper to this (Baker et al., in press), we study the mathematical basis for our model in more detail. In particular, we explain our reasons for modelling a generic fgf8 factor, and we detail the simplifying approximations applied to the model used here that allowed us to predict the sequences of somites formed under local application of FGF8.

Future avenues of exploration lie in several areas. Firstly, in trying to rework the model to use a mechanism better related to the segmentation clock: the somitic factor could be linked to a number of genes, for example, *Mesp2*, but as yet there is no well-established biological basis for the signal. One possible alteration would be to allow the periodic expression of the cycling genes to activate somitic factor production, but only in cells that have reached the determination front and therefore become competent to form somites.

The FGF8 wavefront provides the second avenue for future studies. It has recently been shown that retinoic acid is expressed along the AP axis in a manner opposite to FGF8: high in the somites (anterior) and low in the posterior part of the PSM (Diez del Corral et al., 2003). Findings suggest that the FGF and retinoid pathways are mutually inhibitory and act to control somite formation (Diez del Corral and Storey, 2004).

Lastly, it should be noted that Wnt3a has been postulated to play a major role in somitogenesis: in control of the segmentation clock via Notch signalling; and in control of the determination front via FGF8 expression (Aulehla et al., 2003). This finding suggests a link between the segmentation clock and the FGF8 wavefront and deserves further investigation.

Acknowledgments

Appendix A. Mathematical formulation of the new Clock and Wavefront model

Letting u denote the concentration of somitic factor, v denote the concentration of the diffusive signalling molecule and w denote the concentration of FGF8, we choose to model somite formation using the following non-dimensional model:

$$\frac{\partial u}{\partial t} = \underbrace{\frac{(u+\mu v)^2}{\gamma + u^2}\chi_u}_{\text{Activation by } v \text{ and regulated activation by } u} - \underbrace{u}_{\text{Linear decay}}, \qquad (1)$$

$$\frac{\partial v}{\partial t} = \kappa\left(\underbrace{\frac{\chi_v}{\varepsilon + u}}_{\text{Inhibition by } u} - \underbrace{v}_{\text{Linear decay}}\right) + \underbrace{D_v\frac{\partial^2 v}{\partial x^2}}_{\text{Diffusion}}, \qquad (2)$$

$$\frac{\partial w}{\partial t} = \underbrace{\chi_w}_{\text{Production of } w \text{ in the node}} - \underbrace{\eta w}_{\text{Linear decay}} \qquad (3)$$

$$+ \underbrace{D_w\frac{\partial^2 w}{\partial x^2}}_{\text{Diffusion}},$$

where μ, γ, κ, ε, η, D_v, D_w, w^*, t_s, x_n and c_n are positive constants. Production of u, v and w are controlled by the respective Heaviside functions

$$\chi_u = H(w^* - w), \qquad (4)$$

$$\chi_v = H(t - t_w(w^*, x) - t_s), \qquad (5)$$

$$\chi_w = H(x - x_n - c_n t), \qquad (6)$$

where w^* is the level of FGF8 at the determination front, t_w (w^*, x) is the time at which a cell at x reaches the determination front (i.e. $w(x, t_w) = w^*$), t_s is the period of the segmentation clock, x_n represents the initial position of the tail and c_n represents the rate at which the AP axis is extending. The Heaviside function works like a switch: it is equal to unity when the bracketed expression is positive, and zero otherwise.

The dynamics of the spatially homogeneous equations have been analysed thoroughly in previous work (McInerney et al., 2004). Within a certain parameter regime (which is detailed in the article), the system displays periodic pulses in the signalling molecule as a result of non-linear interactions between the somitic factor u, and the signalling molecule v. These periodic pulses in v lead to coherent rises in the level of somitic factor and the generation of a regular array of somites.

Appendix B. Numerical solution of the model

We solved the above system numerically using the NAG library routine D03PCF, which is designed for non-linear parabolic (including some elliptic) partial differential equations (PDEs) in one spatial variable. The routine is based on the method of lines, using a finite difference approximation to reduce the system of PDEs to a system of ordinary differential equations in the time variable. The resulting system is solved using an implementation of the Backward Differentiation Formula method. The independent variables form a grid: in general, the mesh consisted of 2001 × 2001 points, the output of which was plotted using the Matlab function imagesc. The accuracy of the numerical method was tested by both varying the mesh resolution and the error parameter of the routine (which controls integration in the time direction).

Appendix C. Mathematical formulation of the perturbed Clock and Wavefront model

The modified non-dimensional equations for somite formation in the presence of a local source of FGF8 are:

$$\frac{\partial u}{\partial t} = \frac{(u+\mu v)^2}{\gamma + u^2}\chi_u - u, \qquad (7)$$

$$\frac{\partial v}{\partial t} = \kappa\left(\frac{\chi_v}{\varepsilon + u} - v\right) + D_v\frac{\partial^2 v}{\partial x^2}, \qquad (8)$$

$$\frac{\partial w}{\partial t} = \chi_w + \phi\chi_b - \eta w + D_w \frac{\partial^2 w}{\partial x^2}, \tag{9}$$

where χ_u, χ_v and χ_w are as in Appendix A and $\chi_b = H(\xi - x_b + x)$ $H(\xi + x_b - x)$ represents a source of FGF8 from a bead. x_b is the position of the midpoint of the bead implant and ξ is a measure of the width of the bead (χ_b is non-zero over a region of width 2ξ, centred at x_b).

References

Aulehla, A., Wehrle, C., Brand-Saberi, B., Kemler, R., Gossler, A., Kanzier, B., Herrman, B.G., 2003. Wnt3a plays a major role in the segmentation clock controlling somitogenesis. Dev. Cell 4, 395–406.

Baker, R.E., Schnell, S., Maini, P.K., 2003. Formation of vertebral precursors: past models and future predictions. J. theor. Med. 5, 23–35.

Baker, R.E., Schnell, S., Maini, P.K., in press. A mathematical investigation of a Clock and Wavefront model for somitogenesis. J. Math. Biol. (doi:10.1007/S00285-005-0362-2).

Collier, J.R., McInerney, D., Schnell, S., Maini, P.K., Gavaghan, D.J., Houston, P., Stern, C.D., 2000. A cell cycle model for somitogenesis: mathematical formulation and numerical solution. J. Theor. Biol. 207, 305–316.

Cooke, J., Zeeman, E.C., 1976. A Clock and Wavefront model for control of the number of repeated structures during animal morphogenesis. J. Theor. Biol. 58, 455–476.

Dale, K.J., Pourquié, O., 1997. A clock-work somite. BioEssays 22, 83.

Dale, J.K., Maroto, M., Dequeant, M.-L., Malapert, P., McGrew, M., 2001. Periodic notch inhibition by lunatic fringe underlies the chick segmentation clock. Nature 421, 275–278.

Diez del Corral, R., Olivera-Martinez, I., Goriely, A., Gale, E., Maden, M., Storey, K., 2003. Opposing FGF and retinoid pathways control ventral neural pattern, neuronal differentiation and segmentation during body axis extension. Neuron 40, 65–79.

Diez del Corral, R., Storey, K., 2004. Opposing FGF and retinoid pathways: a signalling switch that controls differentiation and patterning onset in the extending vertebrate body axis. BioEssays 26, 857–869.

Dubrulle, J., Pourquié, O., 2002. From head to tail: links between the segmentation clock and antero-posterior patterning of the embryo. Curr. Opin. Genet. Dev. 5, 519–523.

Dubrulle, J., Pourquié, O., 2004. *fgf8* mRNA decay establishes a gradient that couples axial elongation to patterning in the vertebrate embryo. Nature 427, 419–422.

Dubrulle, J., McGrew, M.J., Pourquié, O., 2001. FGF signalling controls somite boundary position and regulates segmentation clock control of spatiotemporal *Hox* gene activation. Cell 106, 219–232.

Gossler, A., Hrabĕ de Angelis, M., 1998. Somitogenesis. Curr. Top. Dev. Biol. 38, 225–287.

Ishikawa, A., Kitajima, S., Takahashi, Y., Kokubo, H., Kanno, J., Inoue, T., Saga, Y., 2005. Mouse Nkd1, a Wnt antagonist, exhibits oscillatory gene expression in the PSM under the control of Notch signalling. Mech. Dev. 121, 1443–1453.

Lewis, J., 2003. Autoinhibition with transcriptional delay: a simple mechanism for the zebrafish somitogenesis oscillator. Curr. Biol. 13, 1398–1408.

McGrew, M.J., Pourquié, O., 1998. Somitogenesis: segmenting a vertebrate. Curr. Opin. Genet. Dev. 8, 487–493.

McGrew, M.J., Dale, J.K., Fraboulet, S., Pourquié, O., 1998. The lunatic Fringe gene is a target of the molecular clock linked to somite segmentation in avian embryos. Curr. Biol. 8, 979–982.

McInerney, D., Schnell, S., Baker, R.E., Maini, P.K., 2004. A mathematical formulation for the cell cycle model in somitogenesis: parameter constraints and numerical solutions. IMA J. Math. Appl. Med. Biol. 21, 85–113.

Meinhardt, H., 1986. Models of segmentation. In: Bellairs, R., Ede, D.A., Lash, J.W. (Eds.), Somites in Developing Embryos. Plenum Press, New York, pp. 179–189.

Monk, N.A.M., 2003. Oscillatory expression of Hes1, p53 and NF-κB driven by transcriptional time delays. Curr. Biol. 13, 1409–1413.

Palmeirim, I., Henrique, D., Ish-Horowicz, D., Pourquié, O., 1997. Avian *hairy* gene expression identifies a molecular clock linked to vertebrate segmentation and somitogenesis. Cell 91, 639–648.

Pourquié, O., 2003. The segmentation clock: converting embryonic time into spatial pattern. Science 301, 328–330.

Pourquié, O., 2004a. The chick embryo: a leading model for model in somitogenesis studies. Mech. Dev. 121, 1069–1079.

Pourquié, O., Pers. Comm. 2004b.

Primmett, D.R.N., Stern, C.D., Keynes, R.J., 1988. Heat shock causes repeated segmental anomalies in the chick embryo. Development 104, 331–339.

Primmett, D.R.N., Norris, W.E., Carlson, G.J., Keynes, R.J., Stern, C.J., 1989. Periodic segmental anomalies induced by heat shock in the chick embryo are associated with the cell cycle. Development 105, 119–130.

Saga, Y., Takeda, H., 2001. The making of the somite: molecular events in vertebrate segmentation. Nat. Rev., Genet. 2, 835–845.

Schnell, S., Maini, P.K., McInerney, D., Gavaghan, D.J., Houston, P., 2002. Models for pattern formation in somitogenesis: a marriage of cellular and molecular biology. C.R. Biol. 325, 179–189.

Stern, C.D., Fraser, S.E., Keynes, R.J., Primmett, D.R.N., 1988. A cell lineage analysis of segmentation in the chick embryo. Development 104S, 231–244.

Stickney, H.L., Barresi, M.S.J., Devoto, S.H., 2000. Somite development in zebrafish. Dev. Dyn. 219, 287–303.

Stockdale, F.E., Nikovits Jr., W., Christ, B., 2000. Molecular and cellular biology of avian somite development. Dev. Dyn. 219, 304–321.

Tabin, C.J., Johnson, R.L., 2001. Clocks and Hox. Nature 412, 780–781.